Controlling Wake Turbulence

B. S. V. Patnaik and G. W. Wei*

(Received 28 July 2001; published 17 January 2002)

This Letter introduces a control strategy for taming the wake turbulence behind a cylinder. An angular momentum injection scheme is proposed to synchronize the vertical velocity field. We show that the base suction, wake formation length, absolute instability, and the Kármán vortex street are effectively controlled by the angular momentum injection. A control equation is designed to implement the injection. The Navier-Stokes equations, along with the control equation, are solved. The occurrence of a new recirculation free zone is identified.

DOI: 10.1103/PhysRevLett.88.054502 PACS numbers: 47.27.Rc, 05.45.Gg, 05.45.Xt, 47.32.Cc

Since the work by Ott, Grebogi, and Yorke [1], the surge of research on chaos control over the past decade from theory, simulations, and experiments have yielded a wealth of new understanding [2]. Synchronization of chaotic systems such as mechanical, electronic, and chemical systems, as well as solid-state lasers, heart tissues, pattern dynamics, and turbulence in the Ginzburg-Landau equation were studied [3]. Turbulence is one of the most fascinating phenomena in nature. It is of primary importance for many kinetic processes such as molecular chaos and plasma motion, and can cause mechanical failure in many situations. A major goal of turbulence study is to predict and control turbulence so that the phenomenon can be suppressed or enhanced as circumstances dictate in various applications [4].

The objective of this Letter is to introduce a synchronization based angular momentum injection scheme for the control of wake turbulence behind a cylinder. Flow past a bluff body poses a great challenge due to the interaction of three shear layers, i.e., a boundary layer, a separating free shear layer, and a wake. Despite intensive studies [5], much of our understanding of the problem is still in the realm of empiricism and description. Dictated by the Reynolds number, the flow behind a cylinder exhibits a variety of complicated phenomena, such as the transition from a steady pair of eddies to an unsteady vortex shedding in the wake, and the scenario of Kármán vortex street formation, transition, and turbulence. Three possible scenarios have been reported for the occurrence of shear layer instability, for a class of spatially developing flows [6]. The scenario of direct relevance to the present investigation is the shear layer instability of the wake. At a small Reynolds number, a steady pair of eddies in the wake is strictly a supercritical bifurcation of Hopf type and is described by the Ginzburg-Landau equation, which arises in many weakly nonlinear fluid flow systems close to marginal stability. As the Reynolds number increases, the Kármán vortex street develops due to self-sustained hydrodynamic resonance and it goes hand in hand with an absolutely unstable zone and a convectively unstable zone [7]. Resonance occurs when vorticial shedding at the trailing edge of the upstream body is in phase with the vertical velocity induced by the global pressure fluctuation. The absolute instability is dominated by a pure frequency instability and is insensitive to the amplitude of the initial disturbance, whereas for the convective instability, microscopic fluctuations are amplified exponentially while being convected through the system. The region of absolute instability coincides approximately with the recirculating eddies formed behind the cylinder. A further increase in the Reynolds number leads to the onset of wake turbulence, which is manifested in the vortex dislocation. However, we illustrate in this Letter that this instability can be suppressed by an angular momentum injection scheme. The latter effectively changes the base suction, the formation length of the mean recirculation, and the zone of absolutely unstable wake. We investigate the efficacy of the scheme on the spatiotemporal dynamics of the wake. In particular, we are interested in attaining a strictly laminar flow, i.e., a *synchronized state* $\tilde{v}$, which is characterized by the vanishing vertical velocity component. We illustrate that an efficient control is achieved when the vertical velocity is synchronized. The transition from turbulence to synchronization is realized by the inception and growth of a zone, which is free from recirculation. This zone has distinct features as against absolute and convective instability zones.

We consider the problem of flow past a "D" cylinder, as shown in Fig. 1, which is obtained by modifying a square cylinder of the size of $a \times a$. Two circular cylinders of the diameter $\frac{a}{2}$ are cast at the centers of the first and

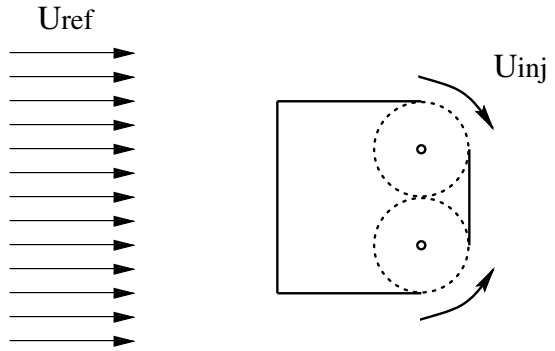

FIG. 1. Flow past a D cylinder with angular momentum injection by two rotating cylinders.

 0031-9007/02/88(5)/054502(4)$20.00

fourth quadrants of the square, and are allowed to rotate in clockwise and anticlockwise fashion, respectively. Their tangential speed on the cylinder surface U_{inj}, is characterized with respect to the incoming reference velocity U_{ref} by the rotation (injection) parameter $\zeta = |U_{\text{inj}}|/|U_{\text{ref}}|$. The entire geometry could be envisioned as the cross section of a three-dimensional (3D) real cylinder with an infinitely long length in the third direction. For a detailed analysis, we resort to a theoretical model.

We invoke the Navier-Stokes equations for a direct numerical simulation (DNS) of flow past the D cylinder. The full Navier-Stokes equations are adequate for both laminar and turbulent flows. However, a 3D DNS study of flow past a cylinder is a challenging task. To illustrate our idea of synchronization and control of wake turbulence and to avoid unnecessary complications, we consider a 2D incompressible flow governed by

$$\frac{\partial \mathbf{v}}{\partial t} + \mathbf{v} \cdot \nabla \mathbf{v} = -\nabla p + \frac{1}{\text{Re}} \nabla^2 \mathbf{v} \tag{1}$$

$$\nabla \cdot \mathbf{v} = 0, \tag{2}$$

where $\mathbf{v}$ is the velocity vector having components $u(x, y, t)$ and $v(x, y, t)$ in the x and y directions, Re is the Reynolds number and p is the pressure field. The above equation was nondimensionalized as, $x = \frac{\bar{x}}{a}$; $y = \frac{\bar{y}}{a}$; $t = \frac{\bar{t}}{a/U_{\text{ref}}}$; $p = \frac{\bar{p}}{\rho U_{\text{ref}}^2}$; $\text{Re} = \frac{U_{\text{ref}} a}{\nu}$. Here, variables with an overbar refer to their corresponding dimensional values, ρ is the density, and ν is the kinematic viscosity of the fluid. We choose a sufficiently large domain size to minimize the undesirable boundary effects. The inflow and exit boundaries are each located at $8a$ and $32a$ towards the fore and aft of the D cylinder, respectively. The far field boundary is located at $8a$ on either side of the central axis. A uniform inflow boundary condition, together with the Neumann boundary condition for the far field and outflow, are applied for the velocity. The no-slip boundary condition is employed for the nonrotational part of the D cylinder. The Neumann boundary condition is also imposed for the pressure at the exit. The Navier-Stokes equations are solved in primitive variables by using the standard fractional step scheme in conjunction with a second order Runge-Kutta scheme for the time integration, and a finite element based Galerkin scheme for the spatial discretization [8]. Three types of grid densities have been employed to verify that the present results are grid independent.

Figure 2 illustrates the impact of the local angular momentum injection on the wake patterns simulated at Re = 200. A streakline technique is utilized for the visualization of the spatiotemporal motion of the flow field. The plot depicts a gradual increment in the value of the injection parameter (ζ) for wake control. When no rotation is imparted to the control cylinders, Kármán vortex street is in its natural and full blown form, which is a waxing

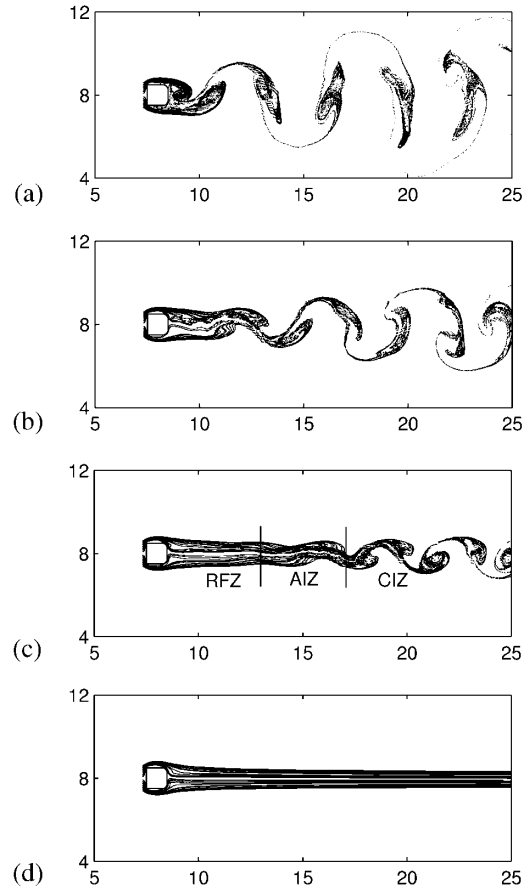

FIG. 2. Streakline plots depicting a gradual wake control by angular momentum injection. (a) $\zeta = 0.0$; (b) $\zeta = 1.0$; (c) $\zeta = 1.25$; (d) $\zeta = 1.5$. The flow domain can be thought of as having been divided into three zones, viz., RFZ: Recirculation Free Zone; AIZ: Absolute Instability Zone; CIZ: Convective Instability Zone.

state, see Fig. 2a. There is a gradual roll up of shear layers at crests and troughs with a mutual connection between all the shed eddies through streaklines, which essentially originate in the near wake. Every shed eddy is ultimately interconnected to every other eddy by its own umbilical chord or thread [9].

Some analytical and experimental studies are available for flow past a circular cylinder [10], establishing the link between vortex shedding and stability theory. The Landau equation was used to study such a perspective. It is established in the literature that the Kármán vortex shedding at low Reynolds numbers is a self-excited limit-cycle oscillation of the near wake, resulting from a global instability. Chomaz *et al.* [6] have postulated that the entire wake region could be described by two zones of instability, viz. absolute and convective. There is a branch off from absolute to convective instability at some downstream location. We surmise that the efficacy of the angular momentum injection essentially depends on the ability to effectively control the base suction behind the cylinder, which in turn leads to changes in the mean recirculation

length, absolute instability zone (AIZ), and the convective instability zone (CIZ). To verify our idea, we set $\zeta = 1.0$. Indeed, we see a waning in the Kármán vortex street as shown in Fig. 2b. Such a reduction in the wake width is associated with an obvious increase in the shedding frequency. Further, it is noted that the AIZ is enlarged due to the increase in the base suction (a reduction in its absolute value) by the injection of angular momentum. Nevertheless, the eddies continue to be fed by circulation from the upstream shear layers. However, with a subsequent increase in the value of the angular momentum injection parameter ($\zeta = 1.25$), we observe a new zone behind the cylinder—the occurrence of a recirculation-free zone (RFZ) just behind the cylinder. As the AIZ is characterized by the eddy recirculation, the existence of the RFZ is verified by the ordered, parallel streaklines. Behind the RFZ, there is still an AIZ and a CIZ, although their sizes are significantly smaller (see Fig. 2c). The target state is achieved at $\zeta = 1.5$, and is depicted in Fig. 2d. Here, only RFZ persists over the entire computational domain, while the two instability zones, AIZ and CIZ completely vanish.

It remains to be proven that a synchronized state has been reached. To monitor the deviation from the target state $\tilde{v}$, we introduce a local variance by a synchronization based coupling between the target state $\tilde{v}$ and the vertical flow field v

$$\sigma^2(x, y) = \frac{1}{s} \int_0^s [v(x, y, t) - \tilde{v}(x, y, t)]^2 \, dt \,, \qquad (3)$$

where s refers to the total time which is much larger compared to the vortex shedding period of the wake. The local variance obtained from several monitored sensor points essentially vanish when $\zeta = 1.5$, while the sensors in the near wake reach the same even at a smaller value of ζ (see Table I).

After performing numerical simulations at specific injection parameters, we design an automatic control scheme to tame the wake turbulence. To measure the degree of synchronization, we define a total variance $\sigma^2(t) = \frac{1}{\int_\Omega dxdy} \int_\Omega [v(x, y, t) - \tilde{v}(x, y, t)]^2 \, dx \, dy$, where Ω denotes the region behind the D cylinder. The total variance determines the rate of change of the injection parameter $\zeta(t)$

$$\frac{\partial \zeta(t)}{\partial t} = C\sigma^2(t) \,. \qquad (4)$$

Equation (4) is referred to as the control equation for the injection of angular momentum, and it is solved simultaneously with the Navier-Stokes equations. This set of coupled equations render an opportunity to monitor the gradual control of the wake dynamics. The initial value of the injection parameters is taken as $\zeta(0) = 0$. We choose a higher Reynolds number ($\mathrm{Re} = 400$) at which the wake turbulence would be dominant without any angular momentum injection. When $\zeta(t)$ reaches a steady state value, the total variance must vanish, which manifests the synchronization.

Figure 3 illustrates the entire simulation process for $\mathrm{Re} = 200$ and $\mathrm{Re} = 400$. In the beginning, both the angular momentum injection parameter $\zeta(t)$ and the total variance $\sigma^2(t)$ start from a quiescent state (zero values). As the fluid flow patterns evolve behind the D cylinder, the instability leads to the onset of shedding in the wake at around $t = 20$. The synchronization coupling gives rise to a positive $\sigma^2(t)$ which in turn feeds back to the control equation and triggers the injection of angular momentum. After the initial buildup, the total variance subsides to a minimum value at around $t = 200$ for $\mathrm{Re} = 200$ ($t = 300$ for $\mathrm{Re} = 400$), both $\zeta(t)$ and $\sigma^2(t)$ gradually approach steady state values. Particularly, the latter reaches a value close to zero, signifying that it has reached the target synchronized state. Here, the value of constant C (chosen as 0.1) assists in the incorporation of gradual change for the rotation parameter. Interestingly, the injection parameter stabilizes at a value close to $\zeta = 1.5$, which is in compliance with the streakline plot depicted in Fig. 2d for $\mathrm{Re} = 200$.

In summary, we have proposed an effective angular momentum injection strategy for the control of spatiotemporal wake dynamics and turbulence behind a cylinder. By means of synchronization coupling, an automatic control equation is constructed and is solved in conjunction with the Navier-Stokes equations for a direct numerical simulation. The spatiotemporal dynamics of the wake is visualized by streakline patterns. A new wake phenomenon, the formation of a recirculation-free zone, is observed. The increase in the angular momentum injection diminishes the zones of absolute and convective instabilities, and

TABLE I. Local variance obtained from the nine sensors located along the central axis of the D cylinder (the coordinates of the sensors are given in the parentheses).

ζ	1 (9.43, 8.0)	2 (10.525, 8.0)	3 (14.905, 8.0)	4 (16.0, 8.0)	5 (20.0, 8.0)	6 (25.0, 8.0)	7 (30.0, 8.0)	8 (35.0, 8.0)	9 (39.0, 8.0)
0.0	13.995	18.585	9.425	8.380	7.365	6.870	6.660	7.190	6.825
0.5	3.625	9.510	7.230	6.560	6.315	5.915	5.275	4.200	4.710
1.00	0.050	0.595	4.685	4.370	3.960	3.225	2.570	1.930	1.910
1.00	0.005	0.040	2.145	2.935	2.970	2.335	1.845	1.375	1.430
1.25	0.000	0.005	0.065	0.620	0.975	0.945	0.665	0.365	0.285
1.50	0.000	0.000	0.000	0.000	0.000	0.000	0.000	0.000	0.000

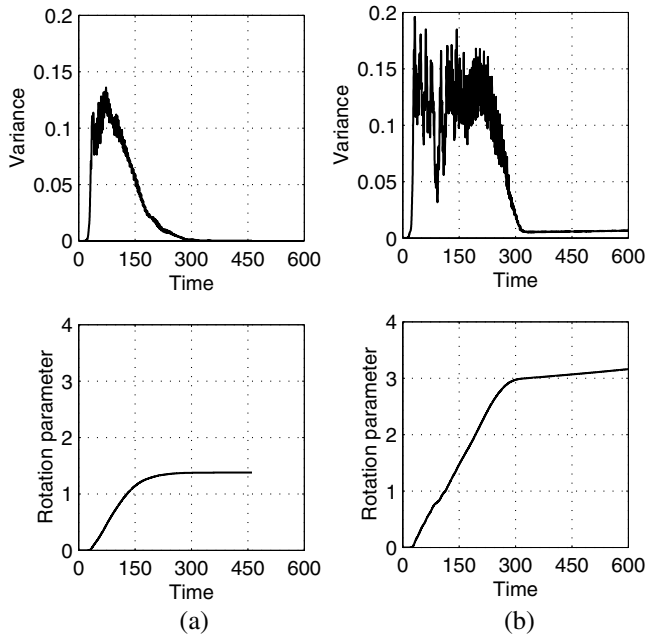

FIG. 3. Temporal evolution of the total variance and its associated rotation (injection) parameter $\zeta(t)$. (a) Re = 200; (b) Re = 400.

enhances the recirculation-free zone. Thus, the wake turbulence could be completely suppressed as the system is synchronized. It is believed that the theoretical findings of this Letter can be realized by experiments and confirmed by 3D simulations.

This work was supported by the National University of Singapore and the National Science and Technology Board of the Republic of Singapore.

*Corresponding author.
Electronic address: cscweigw@nus.edu.sg

[1] E. Ott, C. Grebogi, and J. A. Yorke, Phys. Rev. Lett. **64**, 1196 (1990).

[2] K. Pyragas, Phys. Lett. A **170**, 421 (1992); T. Shinbrot, C. Grebogi, E. Ott, and J. York, Nature (London) **363**, 411 (1993); V. Petrov, V. Gaspar, J. Masere, and K. Showalter, *ibid.* **361**, 240 (1993); G. Hu and Z. Qu, Phys. Rev. Lett. **72**, 68 (1994); D. Auerbach, *ibid.* **72**, 1184 (1994); I. Aranson, H. Levine, and L. Tsimring, *ibid.* **72**, 2561 (1994); P. Y. Wang, P. Xie, J. H. Dai, and H. J. Zhang, *ibid.* **80**, 4669 (1998); K. Myneni, T. A. Barr, N. J. Corron, and S. D. Pethel, *ibid.* **83**, 2175 (1999); G. A. Johnson, M. Locher, and E. R. Hunt, Phys. Rev. E **51**, R1625 (1995); L. Kocarev, U. Parlitz, T. Stojanovski, and P. Janjic, *ibid.* **56**, 1238 (1997); K. Roussopoulos and P. A. Monkewitz, Physica (Amsterdam) **97D**, 264 (1996); S. Boccaletti, C. Grebogi, Y.-C. Lai, H. Mancini, and D. Maza, Phys. Rep. **329**, 103 (2000).

[3] H. Fujisaka and T. Yamada, Prog. Theor. Phys. **69**, 32 (1983); L. M. Pecora and T. L. Carroll, Phys. Rev. Lett. **64**, 821 (1990); W. L. Ditto, S. N. Rauseo, and M. L. Spano, *ibid.* **65**, 3211 (1990); R. Roy and T. W. Murphy, Jr., T. D. Maier, Z. Gills, and E. R. Hunt, *ibid.* **68**, 1259 (1992); M. G. Rosenblum, A. S. Pikovsky, and J. Kurths, *ibid.* **76**, 1804 (1996); A. Neiman, X. Pei, D. Russell, W. Wojtenek, L. Wilkens, F. Moss, H. A. Braun, M. T. Huber, and K. Voigt, *ibid.* **82**, 660 (1999); S. Boccaletti, J. Bragard, F. T. Arecchi, and H. L. Mancini, *ibid.* **83**, 536 (1999); C. M. Ticos and E. Rosa, Jr., W. B. Pardo, J. A. Walkenstein, and M. Monti, *ibid.* **85**, 2929 (2000); E. Allaria, F. T. Arecchi, A. Di Garbo, and R. Meucci, *ibid.* **86**, 791 (2001); G. W. Wei, *ibid.* **86**, 3542 (2001); D. J. DeShazer, R. Breban, E. Ott, and R. Roy, *ibid.* **87**, 044101 (2001); C. Schafer, M. G. Rosenblum, J. Kurths, and H. H. Abel, *ibid.* **392**, 239 (1998); B. Blasius, A. Huppert, and L. Stone, *ibid.* **399**, 354 (1999); C. S. Zhou and C.-H. Lai, Phys. Rev. E **58**, 5188 (1998); S. Boccaletti, L. M. Pecora, and A. Pelaez, *ibid.* **63**, 066219 (2001).

[4] Several reviews have been written on various aspects of turbulence in fluids: experimental, theoretical, and numerical approaches. For a concise and authoritative review with a good number of cross references on fluid turbulence, see K. R. Sreenivasan, Rev. Mod. Phys. **71**, S383 (1999).

[5] Various aspects of the vast amount of literature on bluff body flows have been reviewed by several authors. C. H. K. Williamson, Ann. Rev. Fluid Mech. **28**, 477 (1996); P. Huerre and P. A. Monkewitz, *ibid.* **22**, 473 (1990); H. Oertel, *ibid.* **22**, 539 (1990); P. W. Bearman, *ibid.* **16**, 195 (1984); E. Berger and R. Wille, *ibid.* **4**, 313 (1972); A. Roshko, Int. J. Wind Eng. Ind. Aero Dyn. **49**, 79 (1993).

[6] The three scenarios are the following: extrinsic flows with no resonance, two types of intrinsic flows—one with hydroacoustic resonance and the other with hydrodynamic resonance. The last of the three is of relevance to bluff body wakes. See J. M. Chomaz, P. Huerre, and L. G. Redekopp, Phys. Rev. Lett. **60**, 25 (1988).

[7] The shear layer of the wake is characterized by a change in the instability from locally absolute to a locally convective one at a particular down stream location. Such a transition allows the feedback of temporally growing vorticity waves that propagate up stream and down stream.

[8] A. J. Chorin, Math. Comput. **22**, 745 (1968); B. S. V. Patnaik, P. A. A. Narayana, and K. N. Seetharamu, Int. J. Heat Mass. Transf. **42**, 3495 (1998).

[9] A. E. Perry, M. S. Chong, and T. T. Lim, J. Fluid Mech. **116**, 77 (1982); B. E. Eaton, *ibid.* **180**, 117 (1987).

[10] K. R. Sreenivasan, P. J. Strykowski, and D. J. Olinger, in *Proceedings of the Forum on Unsteady Flow Separation,* edited by K. Ghia (ASME, New York, 1986), p. 1; M. Provansal, C. Mathis, and L. Boyer, J. Fluid Mech. **182**, 1 (1987); P. Plaschko, E. Berger, and R. Peralta-Fabi, Phys. Fluids A **5**, 1718 (1993).